JACS
JOURNAL OF THE AMERICAN CHEMICAL SOCIETY
Article
pubs.acs.org/JACS

Photoinduced Electron Transfer in a Charge-Transfer Complex Formed between Corannulene and $Li^+@C_{60}$ by Concave–Convex $\pi-\pi$ Interactions

Mihoko Yamada,[†] Kei Ohkubo,[†] Mitsuhiko Shionoya,[‡] and Shunichi Fukuzumi*,[†]

[†]Department of Material and Life Science, Graduate School of Engineering, Osaka University, ALCA, Japan Science and Technology (JST), Suita, Osaka 565-0871, Japan

[‡]Department of Chemistry, Graduate School of Science, The University of Tokyo, 7-3-1 Hongo, Bunkyo-ku, Tokyo 113-0033, Japan

Supporting Information

ABSTRACT: A charge-transfer (CT) complex was formed between corannulene ($C_{20}H_{10}$) and lithium ion-encapsulated [60]fullerene ($Li^+@C_{60}$) with the binding constant $K_G = 1.9 \times 10\ M^{-1}$ by concave–convex $\pi-\pi$ CT interactions in benzonitrile at 298 K, exhibiting a broad CT absorption extended to the NIR region. Femotosecond laser excitation of the $C_{20}H_{10}/Li^+@C_{60}$ CT complex resulted in the singlet charge-separated (CS) state, $^1(C_{20}H_{10}^{\bullet+}/Li^+@C_{60}^{\bullet-})$, which decayed with the lifetime of 1.4 ns. Nanosecond laser excitation of $Li^+@C_{60}$ resulted in intermolecular electron transfer (ET) from $C_{20}H_{10}$ to the triplet excited state of $Li^+@C_{60}$ [$^3(Li^+@C_{60})^*$] to produce the triplet CS state $^3(C_{20}H_{10}^{\bullet+}/Li^+@C_{60}^{\bullet-})$. The distance between two electron spins in the triplet CS state was estimated to be 10 Å from the zero-field splitting pattern observed by EPR measurements at 4 K. The triplet CS state decayed to the ground state via intramolecular back electron transfer (BET). The CS lifetime was determined to be 240 μs in benzonitrile at 298 K. The temperature dependence of the rate constant of BET afforded the reorganization energy ($\lambda = 1.04$ eV) and the electronic coupling term ($V = 0.0080\ cm^{-1}$). The long lifetime of triplet CS state results from the spin-forbidden BET process and a small V value.

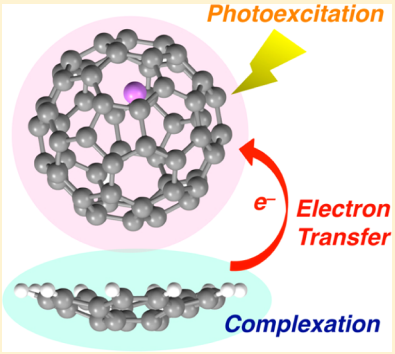

INTRODUCTION

In the photosynthetic reaction center, a long-lived charge-separated (CS) state is attained by photoinduced charge separation processes to convert solar energy to chemical energy.[1] Many electron donor–acceptor (D–A) systems have been designed and investigated as chemical models of the photosynthetic reaction center to attain long-lived CS states.[2−6] In particular, fullerenes have been widely used as efficient π-electron acceptors due to the small reorganization energy, which results from the highly delocalized π-electrons over the three-dimensional π-sphere.[7,8] Until now, a large variety of covalent and noncovalent D–A systems using fullerenes as electron acceptors have been reported, and the photophysical properties of these D–A materials have been investigated both in solution and/or in the solid state as well as their use as active components in photovoltaic devices.[2,5−7,9−13]

The simplest noncovalent D–A systems are derived from charge-transfer (CT) interactions between D and A molecules. According to Mulliken CT theory, the CT interaction in the ground state increases with decreasing the energy difference between the HOMO of D and LUMO of A and also with increasing the orbital overlap between the HOMO and LUMO.[14] Thus, there are many examples of CT complexes formed between relatively strong electron donors such as π-extended tetrathiafulvalene derivatives and fullerenes.[15−17] CT interactions are known to be enhanced by concave–convex $\pi-\pi$ interactions between π-electron donors with curved π-surfaces and fullerenes.[18−24]

Corannulene ($C_{20}H_{10}$),[25−27] a substructure of C_{60}, is one of the smallest curved π-compounds with nonequivalent concave and convex curved π-surfaces, exhibiting bowl-to-bowl inversion behavior,[25c,28] dipole moment,[29] and a variety of coordination sites on both sides.[30] The role of corannulene and its derivatives as a buckyball catcher derived from the curved π-surface which geometrically fits the surface of C_{60} has attracted great attention especially in the field of theoretical and supramolecular chemistry.[31] So far, cocrystal of corannulene and C_{60} in solid state and interaction between corannulene and $C_{60}^{\bullet+}$ in the gas phase have been reported to exhibit the availability of corannulene to catch C_{60} as expected from theoretical calculations.[32] However, CT interactions between corannulene and fullerenes in solution have yet to be reported. No photodynamics of corannulene with fullerenes has been reported, either.[33]

We report herein construction of an electron D–A CT system composed of corannulene and $Li^+@C_{60}$, with concave–convex $\pi-\pi$ CT interactions between the two curved π-surfaces. It should be noted that there was much less CT interaction between corannulene and C_{60}. The use of $Li^+@C_{60}$,

Received: May 29, 2014
Published: August 28, 2014

dx.doi.org/10.1021/ja505391x | J. Am. Chem. Soc. 2014, 136, 13240−13248

which is a much stronger electron acceptor than C_{60},[34] has made it possible to observe the significant CT interaction with corannulene. We have also examined the detailed photodynamics of the CT complex formed between corannulene and $Li^+@C_{60}$ and also intermolecular photoinduced electron transfer (ET) from corannulene to the triplet excited state of $Li^+@C_{60}$ to produce the long-lived triplet CS state. It should also be noted that no such triplet CS state was observed when $Li^+@C_{60}$ was replaced by C_{60}.

RESULTS AND DISCUSSION

A CT Complex Formed between $Li^+@C_{60}$ and $C_{20}H_{10}$. New broad absorption bands were observed in the vis-NIR region upon addition of corannulene ($C_{20}H_{10}$) to a benzonitrile (PhCN) solution of $Li^+@C_{60}PF_6^-$ at 298 K as shown in Figure 1. Because neither $C_{20}H_{10}$ nor $Li^+@C_{60}PF_6^-$ showed NIR

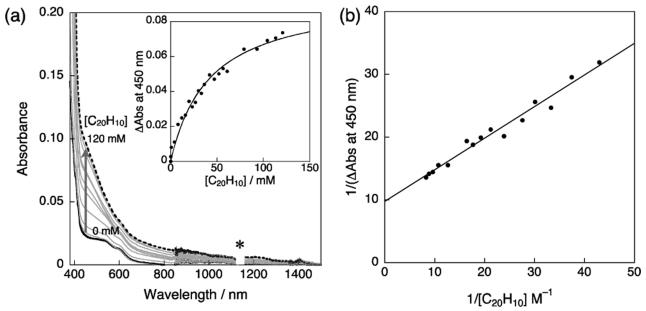

Figure 1. (a) UV-vis-NIR absorption spectra of $Li^+@C_{60}PF_6^-$ (0.10 mM) in the presence of $C_{20}H_{10}$ (from 0 to 120 mM) in PhCN at 298 K (2 mm cell path length). Inset: Plot of ΔAbs at 450 nm vs concentration of $C_{20}H_{10}$ ($[C_{20}H_{10}]$). *: The vibrational absorption due to the solvent is cut off. (b) Plot of ΔAbs^{-1} vs $[C_{20}H_{10}]^{-1}$.

absorption bands in MeCN (Figures S1 and S2 in Supporting Information (SI)), the new vis-NIR absorption bands are ascribed to CT bands from $C_{20}H_{10}$ to $Li^+@C_{60}PF_6^-$ in the electron donor–acceptor (EDA) complex. The CT absorbance was enhanced with increasing concentration of $C_{20}H_{10}$ to approach a constant value as shown in the inset of Figure 1a. Such a saturation behavior indicates formation of the EDA complex between $C_{20}H_{10}$ and $Li^+@C_{60}PF_6^-$ with 1:1 stoichiometry (Scheme 1). The formation constant (K_G) of the EDA complex at the ground state was determined to be $(1.9 \pm 0.1) \times 10\ M^{-1}$ at 298 K by a Benesi–Hildebrand plot (Figure 1b) according to eq 1:[35]

$$\frac{[Li^+@C_{60}]_0}{\Delta Abs} = \frac{1}{\varepsilon K_G [C_{20}H_{10}]_0} + \frac{1}{\varepsilon} \quad (1)$$

where $[Li^+@C_{60}]_0$ and $[C_{20}H_{10}]_0$ are the initial concentrations of $Li^+@C_{60}$ and $C_{20}H_{10}$, respectively, ΔAbs is the increased absorbance of the EDA complex at 450 nm, and ε is the molar extinction coefficient of the EDA complex.

Formation of the EDA complex between $C_{20}H_{10}$ and $Li^+@C_{60}PF_6^-$ was also confirmed by the change in the ^7Li NMR of $Li^+@C_{60}PF_6^-$ (1.0 mM) after addition of $C_{20}H_{10}$ (95 mM) in *o*-dichlorobenzene-d_4 at 298 K. The observed 0.66 ppm upfield shift indicates that the EDA complex between $C_{20}H_{10}$ and $Li^+@C_{60}PF_6^-$ is stabilized by CT interaction between $C_{20}H_{10}$ and $Li^+@C_{60}PF_6^-$, which results in an increase in the electron density of Li^+. The K_G value was also determined from the NMR titration in *o*-dichlorobenzene-d_4 to be $(2.4 \pm 0.5) \times 10$ M^{-1} by the Benesi–Hildebrand plot (Figures S3 and S4 in SI), which agrees within experimental error with the value obtained by the absorption change in Figure 1b.

Scheme 1. Formation of $C_{20}H_{10}/Li^+@C_{60}$ CT Complex in the Ground and Excited States

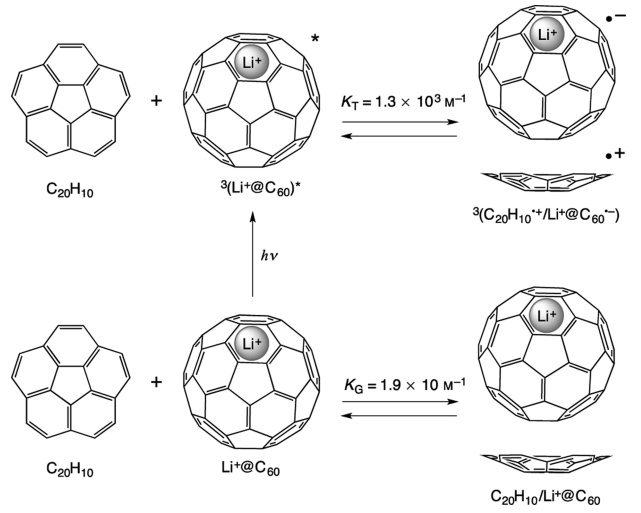

When $Li^+@C_{60}$ was replaced by C_{60}, CT absorption was also observed by addition of $C_{20}H_{10}$ to a PhCN solution of C_{60} as shown in Figure S5 (SI), where the CT absorption of the $C_{20}H_{10}/C_{60}$ complex is much less pronounced. The K_G value of $C_{20}H_{10}/C_{60}$ was estimated to be $\ll 1\ M^{-1}$ from no saturation behavior in the presence of up to 120 mM $C_{20}H_{10}$ in Figure S5 (SI), which is significantly smaller than that of the $C_{20}H_{10}/Li^+@C_{60}$ complex $(1.9 \pm 0.1) \times 10\ M^{-1}$, because C_{60} is a much weaker electron acceptor than $Li^+@C_{60}$.[34]

To predict the structure of the $C_{20}H_{10}/Li^+@C_{60}$ complex, the theoretical calculations were performed by DFT at the B3LYP/6-31G(d) level of theory.[36] The optimized structure is shown in Figure 2. The $C_{20}H_{10}$ moiety has the concave–convex π–π interaction with the $Li^+@C_{60}$ moiety by using their curved π-surfaces. The concave–convex π–π CT interaction could more stabilize the CT complex than the convex–convex π–π interaction because of maximized overlapping area of HOMO

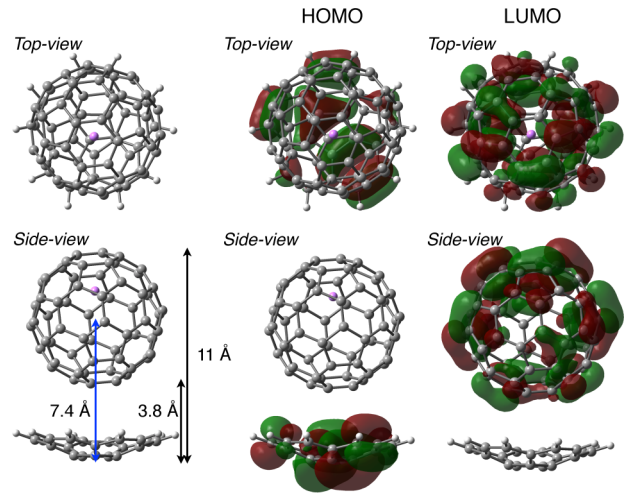

Figure 2. Optimized structure, HOMO, and LUMO of $C_{20}H_{10}/Li^+@C_{60}$ CT complex calculated by a DFT method at the B3LYP/6-31G(d) level.

dx.doi.org/10.1021/ja505391x | J. Am. Chem. Soc. 2014, 136, 13240–13248

of $C_{20}H_{10}$ and LUMO of $Li^+@C_{60}$. The HOMO and LUMO are localized at the $C_{20}H_{10}$ and $Li^+@C_{60}$ moieties, respectively (Figure 2).

Electrochemical Measurements of the $C_{20}H_{10}/Li^+@C_{60}$ Complex. The energetics of photoinduced ET from $C_{20}H_{10}$ to $Li^+@C_{60}$ were determined by cyclic voltammetry (CV) and second harmonic ac voltammetry (SHACV) measurements together with the emission energies of $C_{20}H_{10}$ to $Li^+@C_{60}$.[37] The driving force of charge recombination (CR) from $Li^+@C_{60}^{\bullet-}$ to $C_{20}H_{10}^{\bullet+}$, which corresponds to the Gibbs free energy of intermolecular ET from $C_{20}H_{10}$ to $Li^+@C_{60}$, was determined to be 1.65 eV from the redox potential difference between the one-electron oxidation potential of $C_{20}H_{10}$ (1.81 V vs SCE) and the one-electron reduction potential of $Li^+@C_{60}$ (0.16 V vs SCE) in Figure 3.

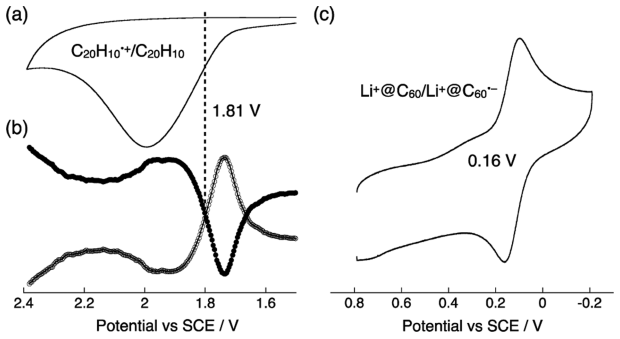

Figure 3. (a) CV and (b) SHACV of $C_{20}H_{10}$ (3.5 mM) with $Li^+@C_{60}PF_6^-$ (1.0 mM) in deaerated PhCN containing *n*-Bu_4NPF_6 (0.10 M) with a platinum disk electrode (i.d. 1.6 mm) at 298 K. (c) CV of $Li^+@C_{60}PF_6^-$ (1.0 mM) with $C_{20}H_{10}$ (3.5 mM) in deaerated PhCN containing *n*-Bu_4NPF_6 (0.10 M) with a platinum disk electrode (i.d. 1.6 mm) at 298 K. Scan rate: 100 mV s^{-1} for CV and 4 mV s^{-1} for SHACV.

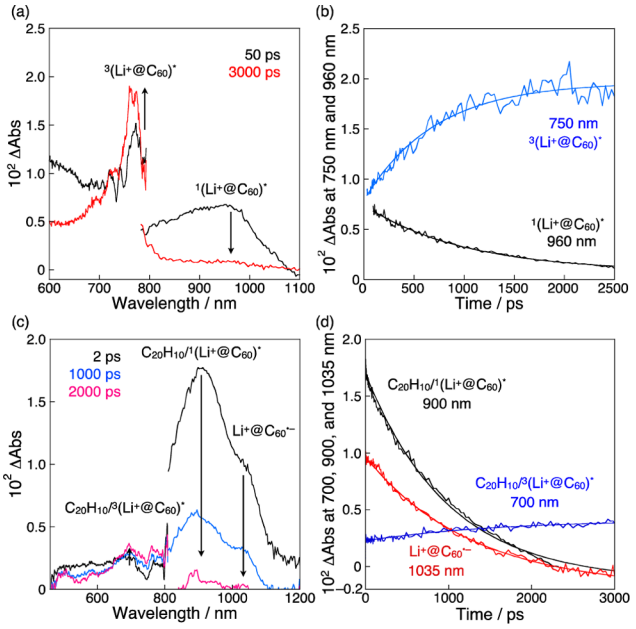

Figure 4. (a) Transient absorption spectra of a PhCN solution containing $C_{20}H_{10}$ (50 μM) and $Li^+@C_{60}PF_6^-$ (500 μM) at 298 K measured at 50 ps (black) and 3000 ps (red) after laser excitation at 393 nm. (b) Decay time profile of absorbance at 960 nm due to $^1(Li^+@C_{60})^*$ and rise time profile of absorbance at 750 nm due to $^3(Li^+@C_{60})^*$. (c) Transient absorption spectra of $C_{20}H_{10}$ (125 mM) and $Li^+@C_{60}PF_6^-$ (500 μM) in PhCN at 298 K measured at 2 ps (black), 1000 ps (blue), and 2000 ps (pink) after laser excitation at 450 nm. (d) Decay time profiles of absorbance at 700, 900, and 1035 nm due to $C_{20}H_{10}/^3(Li^+@C_{60})^*$, $C_{20}H_{10}/^1(Li^+@C_{60})^*$, and $Li^+@C_{60}^{\bullet-}$, respectively. The solid line for the decay profile of 1035 nm was drawn by two-exponential rise and decay curve fitting with the equation of ΔAbs at 1035 nm = $A_1 \exp(-k_{BETC}t) - A_2 \exp(-k_{ISCC}t) + C$. The value of k_{ISCC} is $(6 \pm 1) \times 10^8$ s^{-1}. The values of k_{BETC}, A_1, A_2, and C are listed in Table S1 in SI.

The excited-state energy of $^1(Li^+@C_{60})^*$ was determined previously from the absorption and fluorescence maxima to be 1.94 eV, whereas the triplet energy of $^3(Li^+@C_{60})^*$ was determined from the phosphorescence maximum to be 1.53 eV.[38] The excited-state energies of $^1(C_{20}H_{10})^*$ and $^3(C_{20}H_{10})^*$ were also determined from the absorption and emission maxima to be 3.63 and 2.43 eV, respectively (Figures S1, S6, and S7 in SI). The excited-state energies of $^1(Li^+@C_{60})^*$, $^1(C_{20}H_{10})^*$, and $^3(C_{20}H_{10})^*$ are higher than the energy of the CS state, suggesting that photoinduced ET from each of the excited states is energetically favorable.

Photoinduced Charge Separation in the $C_{20}H_{10}/Li^+@C_{60}$ CT Complex. The transient absorption spectra of PhCN solutions of $C_{20}H_{10}$ and $Li^+@C_{60}$ were measured by femtosecond laser flash photolysis as shown in Figure 4. When formation of the EDA complex is negligible with a small concentration of $C_{20}H_{10}$ (50 μM), a transient absorption band was observed at 960 nm due to the singlet excited state [$^1(Li^+@C_{60})^*$] at 50 ps after femtosecond laser excitation (Figure 4a). The decay of absorbance at 960 nm was accompanied by an increase in the absorption band at 750 nm due to the triplet excited state [$^3(Li^+@C_{60})^*$], which indicates the intersystem crossing (ISC) from $^1(Li^+@C_{60})^*$ to $^3(Li^+@C_{60})^*$. The rate constant of the ISC (k_{ISC}) was determined from the decay of $^1(Li^+@C_{60})^*$ at 960 nm to be $(9.9 \pm 0.5) \times 10^8$ s^{-1}, which is similar to the reported value (8.9×10^8 s^{-1}).[39] Thus, no intermolecular ET from $C_{20}H_{10}$ to $^1(Li^+@C_{60})^*$ occurred to produce the singlet CS state.

When more than 70% of $Li^+@C_{60}$ forms the EDA complex with much excess $C_{20}H_{10}$ in the ground state, femtosecond laser excitation of the $C_{20}H_{10}/Li^+@C_{60}$ complex resulted in appearance of transient absorption bands at 900 and 1035 nm at 2 ps and a broad band in the range from 650 to 800 nm at 2000 ps (Figure 4c). The transient absorption band at 900 nm assigned to $^1(Li^+@C_{60})^*$ in the $C_{20}H_{10}/Li^+@C_{60}$ complex is blue-shifted as compared with that due to free $^1(Li^+@C_{60})^*$, because the ground state of the $C_{20}H_{10}/Li^+@C_{60}$ complex is stabilized by the CT interaction, whereas the excited state is destabilized by the CT interaction according to the Mulliken CT theory.[40] The transient absorption band at 700 nm assigned to $^3(Li^+@C_{60})^*$ in the $C_{20}H_{10}/Li^+@C_{60}$ complex by ISC process is significantly weaker than that of free $^3(Li^+@C_{60})^*$. This may result from the competing ET process from $C_{20}H_{10}$ to $^1(Li^+@C_{60})^*$ to the singlet CS state [$^1(C_{20}H_{10}^{\bullet+}/Li^+@C_{60}^{\bullet-})$]. The shoulder absorption at 1035 nm is assigned to the absorption due to $Li^+@C_{60}^{\bullet-}$ in the singlet CS state. Thus, photoexcitation of the $C_{20}H_{10}/Li^+@C_{60}$ complex resulted in formation of the singlet CS state. The observed decay of absorbance at 900 nm due to $C_{20}H_{10}/^1(Li^+@C_{60})^*$ results from both the ISC process to $C_{20}H_{10}/^3(Li^+@C_{60})^*$ and the competitive formation of the singlet CS state $^1(C_{20}H_{10}^{\bullet+}/Li^+@C_{60}^{\bullet-})$ (Figure 4d). The rate constant of ISC of the

dx.doi.org/10.1021/ja505391x | J. Am. Chem. Soc. 2014, 136, 13240−13248

complex (k_{ISCC}) was determined to be $(6 \pm 1) \times 10^8$ s^{-1} from the rise of absorbance at 700 nm due to $C_{20}H_{10}/^3(Li^+@C_{60})^*$, which is smaller than that of the free $Li^+@C_{60}$ [$k_{ISC} = (9.9 \pm 0.5) \times 10^8$ s^{-1}]. The observed decay constant of absorbance at 900 nm due to $C_{20}H_{10}/^1(Li^+@C_{60})^*$ was determined to be $(1.0 \pm 0.1) \times 10^9$ s^{-1}, which is also smaller than the k_{ISCC} value [$(6 \pm 1) \times 10^8$ s^{-1}]. The difference between the decay rate constant at 900 nm and the k_{ISCC} value [$(4 \pm 1) \times 10^8$ s^{-1}] corresponds to the rate constant of electron transfer from $C_{20}H_{10}$ to $^1(Li^+@C_{60})^*$ to produce the singlet CS state in addition to the CS state produced upon the CT excitation. The rate constant of back electron transfer (BET) of the singlet CS state (k_{BETC}) was determined by fitting the decay time profile of absorbance at 1035 nm due to $Li^+@C_{60}^{\bullet-}$ by two exponentials (one is formation of the CS state and the other is decay of the CS state) to be $(7.4 \pm 0.1) \times 10^8$ s^{-1} (lifetime: 1.4 ± 0.1 ns). Thus, the rate constant of formation of the singlet CS state [$(4 \pm 1) \times 10^8$ s^{-1}] is smaller than that of the decay to the ground state.

The transient absorption spectra of PhCN solutions of $C_{20}H_{10}$ and C_{60} were also measured by femtosecond laser flash photolysis. In the presence of a small concentration of $C_{20}H_{10}$ (50 μM), only intersystem crossing from $^1C_{60}^*$ to $^3C_{60}^*$ was observed after femtosecond laser excitation at 393 nm (Figure S8a in SI) with the rate constant of $(8.7 \pm 0.3) \times 10^8$ s^{-1} (Figure S8b in SI), which agrees with the fluorescence lifetime of C_{60}.[41] In the presence of a large concentration of $C_{20}H_{10}$ (125 mM), however, no transient absorption was observed after femtosecond laser excitation at 450 nm due to the absence of the CT band (Figure S8c in SI) in contrast with the case of $Li^+@C_{60}$ (Figure 4c).

Intermolecular Photoinduced Charge Separation from $C_{20}H_{10}$ to $^3(Li^+@C_{60})^*$ to the Triplet CS State. In contrast to the case of the singlet excited state [$^1(Li^+@C_{60})^*$], the triplet excited state [$^3(Li^+@C_{60})^*$] can undergo intermolecular ET from $C_{20}H_{10}$ to produce the triplet CS state [$^3(C_{20}H_{10}^{\bullet+}/Li^+@C_{60}^{\bullet-})$] as shown in Figure 5, where the decay of the transient absorption band at 750 nm due to $^3(Li^+@C_{60})^*$ observed at 4 μs after nanosecond laser excitation of a PhCN solution of $C_{20}H_{10}$ and $Li^+@C_{60}$ is accompanied by appearance of the absorption band at 1035 nm due to $Li^+@C_{60}^{\bullet-}$ and also the absorption band at 500 nm due to $C_{20}H_{10}^{\bullet+}$.[42]

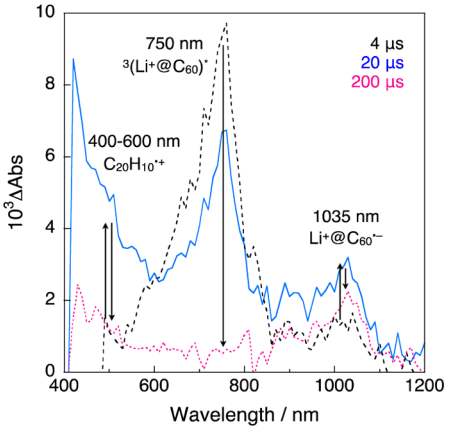

Figure 5. Transient absorption spectra of a PhCN solution containing $C_{20}H_{10}$ (3.5 mM) and $Li^+@C_{60}PF_6^-$ (0.1 mM) taken at 4 (black), 20 (blue), and 200 (pink) μs after laser excitation at 355 nm with 5 mJ $pulse^{-1}$ laser intensity.

The decay rate of absorbance at 750 nm due to $^3(Li^+@C_{60})^*$ coincides with the rise rate of absorbance at 1035 nm due to $Li^+@C_{60}^{\bullet-}$ to produce the triplet CS state (Figure 6a). The

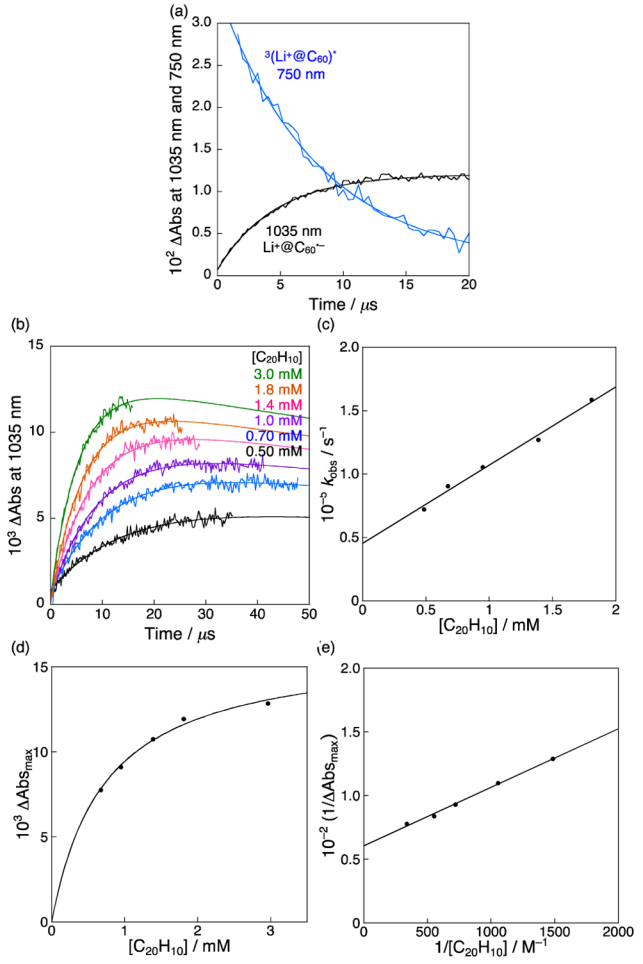

Figure 6. (a) Decay and rise time profiles of absorbance at 750 nm due to $^3(Li^+@C_{60})^*$ and 1035 nm due to $Li^+@C_{60}^{\bullet-}$ after nanosecond laser excitation at 532 nm with 7 mJ $pulse^{-1}$ laser intensity of a PhCN solution of $Li^+@C_{60}PF_6^-$ (0.10 mM) with $C_{20}H_{10}$ (3.0 mM) at 298 K. (b) Time profiles of absorbance at 1035 nm due to $Li^+@C_{60}^{\bullet-}$ using various concentrations of $C_{20}H_{10}$ (0.50, 0.70, 1.0, 1.4, 1.8, 3.0 mM). Solid lines were drawn by double-exponential rise and decay curve fitting with the equation of ΔAbs at 1035 nm $= -A_1 \exp(-k_{obs}t) + A_1 \exp(-k_d t) + C$. The values of k_{obs}, k_d, A_1, and C are listed in Table S2 in SI. (c) Plot of k_{obs} vs concentration of $C_{20}H_{10}$. (d) Plot of Abs_{max} vs concentration of $C_{20}H_{10}$. (e) Benesi–Hildebrand plot of $1/\Delta Abs_{max}$ vs $1/[C_{20}H_{10}]$.

formation of the triplet CS state is followed by the decay of the CS state as shown in Figure 6b, where the rates of formation and decay of the triplet CS state were well simulated by two exponentials. The rate constant of photoinduced ET from $C_{20}H_{10}$ to $^3(Li^+@C_{60})^*$ increased linearly with increasing concentration of $C_{20}H_{10}$ (Figure 6c), whereas the maximum absorbance (Abs_{max}) at 1035 nm due to the triplet CS state increased with increasing concentration of $C_{20}H_{10}$ to approach a constant value (Figure 6d). These results indicate that photoinduced ET from $C_{20}H_{10}$ to $^3(Li^+@C_{60})^*$ to produce the

dx.doi.org/10.1021/ja505391x | J. Am. Chem. Soc. 2014, 136, 13240–13248

triplet CS state is in equilibrium with the BET to regenerate the reactant pair as shown in Scheme 2.

Scheme 2

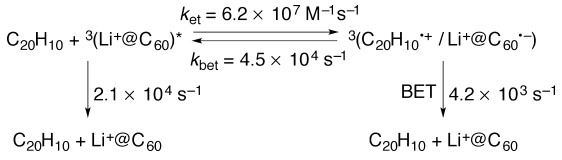

According to Scheme 2, the observed rate constant (k_{obs}) of formation of the triple CS state is given by eq 2:

$$k_{obs} = k_{et}[C_{20}H_{10}] + k_{bet} \quad (2)$$

where k_{et} is the rate constant of ET from $C_{20}H_{10}$ to ${}^3(Li^+@C_{60})^*$ and k_{bet} is the BET to regenerate ${}^3(Li^+@C_{60})^*$. From the slope and intercept of the linear plot in Figure 6c, the formation constant of the triplet CS state ($K_T = k_{et}/k_{bet}$) was determined to be $(1.4 \pm 0.1) \times 10^3\ M^{-1}$. The virtually same K_T value [$(1.2 \pm 0.2) \times 10^3\ M^{-1}$] was obtained from the dependence of the observed rate constant of the decay of ${}^3(Li^+@C_{60})^*$ instead of formation of the triplet CS state (Figure S9 in SI).

The K_T value was also determined from the dependence of Abs_{max} on $[C_{20}H_{10}]$ using eq 3:

$$\frac{[Li^+@C_{60}]_0}{\Delta Abs_{max}} = \frac{1}{\varepsilon_{max} K_T [C_{20}H_{10}]_0} + \frac{1}{\varepsilon_{max}} \quad (3)$$

where ε_{max} is the molar extinction coefficient of absorbance at 1035 nm due to $Li^+@C_{60}^{\bullet-}$. The K_T value was determined from the slope and intercept of the Benesi–Hildebrand plot of ${}^3(Li^+@C_{60})^*$ in Figure 6e to be $(1.3 \pm 0.1) \times 10^3\ M^{-1}$, which agrees well with the value obtained from eq 2. The K_T value of ${}^3(Li^+@C_{60})^*$ to produce the triplet CS state with $C_{20}H_{10}$ is much larger than the K_G value of the ground state of $Li^+@C_{60}$ to form the CT complex with $C_{20}H_{10}$ [$(1.9 \pm 0.1) \times 10\ M^{-1}$] (*vide supra*).

The Gibbs free energy change of formation of the triplet CS state from ${}^3(Li^+@C_{60})^*$ (ΔG_{TCS}) is determined from the K_T value using eq 4 to be −0.18 eV. On the other hand, the Gibbs

$$\Delta G_{TCS} = -RT \ln K \quad (4)$$

free energy change of ET from $C_{20}H_{10}$ to ${}^3(Li^+@C_{60})^*$ (ΔG_{et}) to produce separated radical ion pair ($C_{20}H_{10}^{\bullet+}$ and $Li^+@C_{60}^{\bullet-}$) is determined from the E_{ox} value of $C_{20}H_{10}$ and the E_{red}* value of ${}^3(Li^+@C_{60})^*$ using eq 5 to be +0.12 eV. The energy of the

$$\Delta G_{ET} = -e(E_{ox} - E_{red}^*) \quad (5)$$

triplet CS state, which corresponds to the Gibbs free energy change of BET (ΔG_{BET}), was determined using eq 4 and the triplet energy of ${}^3(Li^+@C_{60})^*$ to be +1.35 eV, which is by 0.18 eV lower than the excitation energy of ${}^3(Li^+@C_{60})^*$.

When $Li^+@C_{60}$ was replaced by C_{60}, no ET from $C_{20}H_{10}$ to ${}^3C_{60}^*$ was observed (Figure S10 in SI), because the ΔG_{TCS} value is estimated to be largely positive (+0.53 eV) due to the much less positive E_{red}* value of C_{60} (1.14 V vs SCE) as compared with the E_{red}* value of $Li^+@C_{60}$ (1.67 V vs SCE).[38,43] Thus, formation of the triplet CS state with corannulene was made possible only by using $Li^+@C_{60}$ which is a much stronger electron acceptor than C_{60}.

Long Lifetime of the Triplet CS State. The lifetime of the triplet CS state produced by intermolecular ET from $C_{20}H_{10}$ to ${}^3(Li^+@C_{60})^*$ was determined from the decay time profile of the absorption band at 1035 nm due to $Li^+@C_{60}^{\bullet-}$ in PhCN (Figure 7). The decay rate constant was determined from the

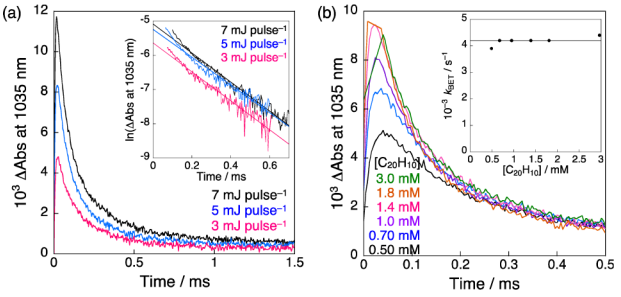

Figure 7. (a) Decay time profiles of transient absorbance at 1035 nm after laser excitation with various laser intensities (3, 5, 7 mJ pulse^{-1}) of a PhCN solution containing $C_{20}H_{10}$ (3.0 mM) and $Li^+@C_{60}PF_6^-$ (0.1 mM) at 298 K. Inset: First-order plots. (b) Decay time profiles of absorbance at 1035 nm after laser excitation of PhCN solutions containing $Li^+@C_{60}PF_6^-$ (0.10 mM) with various concentrations (0.50, 0.70, 1.0, 1.4, 1.8, 3.0 mM) of $C_{20}H_{10}$. Excitation wavelength is 532 nm (7 mJ pulse^{-1} laser intensity). Inset: Plot of k_{BET} vs $[C_{20}H_{10}]$.

first-order plot shown in the inset of Figure 7. The lifetime of the triplet CS state was determined to be 240 μs at 298 K. We also examined the decay rate constant using various different laser intensities to distinguish between intermolecular and intramolecular CR processes. The first-order plots afforded linear correlations with the same slope irrespective of different laser intensity. In addition, no dependence of the decay rate constant on concentration of $C_{20}H_{10}$ was observed as shown in Figure 7b. Thus, there is virtually no contribution from the intermolecular CR process from $Li^+@C_{60}^{\bullet-}$ to $C_{20}H_{10}^{\bullet+}$ and the triplet radical ion pair [${}^3(C_{20}H_{10}^{\bullet+}/Li^+@C_{60}^{\bullet-})$] stays in contact from BET to the ground state.

The rate constant of intramolecular BET (k_{BET}) exhibited small temperature dependence as shown in Figure 8. The k_{BET} values at various temperatures were determined from the slope

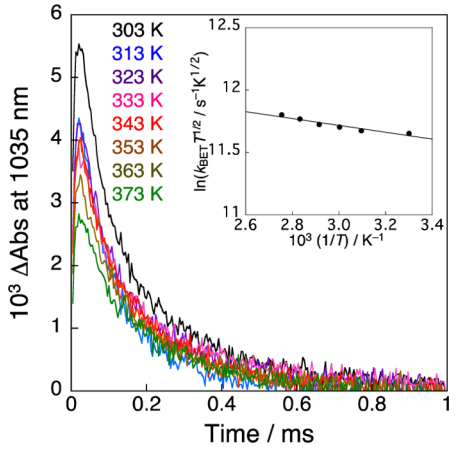

Figure 8. Decay time profiles of absorbance at 1035 nm observed after laser excitation of a deaerated PhCN solution at various temperatures (303–373 K). Excitation wavelength is 355 nm with 5 mJ pulse^{-1} intensity. The solution contains $C_{20}H_{10}$ (3.5 mM) and $Li^+@C_{60}$ (0.1 mM). Inset: Plots of $\ln(k_{BET}T^{1/2})$ vs T^{-1} for the intramolecular BET between $C_{20}H_{10}$ and $Li^+@C_{60}$.

dx.doi.org/10.1021/ja505391x | J. Am. Chem. Soc. 2014, 136, 13240–13248

of the first-order plot in Figure S11 in SI. The temperature dependence of k_{BET} was fitted by the Marcus equation for nonadiabatic ET (eq 6):[44,45]

$$\ln(k_{BET}T^{1/2}) = \ln\left(\frac{2\pi^{3/2}V^2}{h(\lambda k_B)^{1/2}}\right) - \frac{(\Delta G_{BET} + \lambda)^2}{4\lambda k_B T} \quad (6)$$

where T is the temperature, V is the electronic coupling constant, λ is the reorganization energy, ΔG_{BET} is the Gibbs free energy change of BET, k_B is the Boltzmann constant, and h is Planck's constant. Equation 6 predicts a linear correlation between $\ln(k_{BET}T^{1/2})$ and T^{-1}. The plot of $\ln(k_{BET}T^{1/2})$ vs T^{-1} for the intramolecular BET in the temperature range from 303 to 373 K gave linear correlations as shown in the inset of Figure 8. From the slope, intercept, and the driving force $-\Delta G_{BET}$ (1.35 eV), the λ and V values were determined to be λ = 1.04 eV and V = 0.0080 cm^{-1} for BET. This extremely small V values compared to those reported for many other charge separation systems might result from the spin-forbidden process (Scheme 2).[39,46−48]

The long-lived triplet CS state was detected by the EPR with photoirradiation at low temperature in a PhCN solution of $C_{20}H_{10}$ and Li$^+$@C_{60}, and quenched at 4 K as shown in Figure 9. The spin−spin interaction in the triplet radical ion pair was

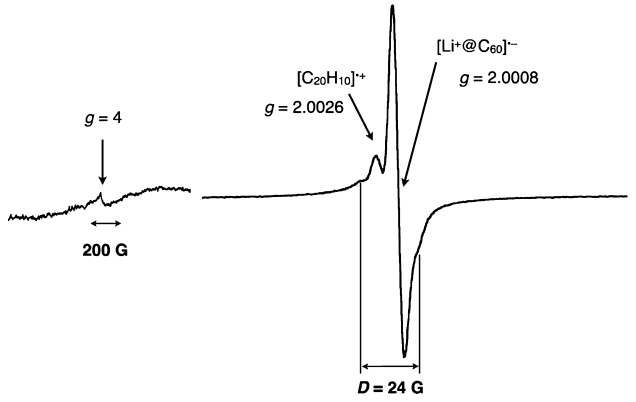

Figure 9. EPR spectra of the triplet CS state [^{3}($C_{20}H_{10}^{\bullet+}$/Li$^+$@$C_{60}^{\bullet-}$)] in PhCN generated by photoirradiation of a solution containing $C_{20}H_{10}$ (5.0 mM) and Li$^+$@$C_{60}PF_6^-$ (0.5 mM) using a high-pressure Hg lamp at 4 K.

clearly observed at 4 K with the fine structure due to the triplet CS state at g = 2 and a triplet signal at g = 4. The signal at g = 2 is composed of signals mainly due to $C_{20}H_{10}^{\bullet+}$ and Li$^+$@$C_{60}^{\bullet-}$, respectively, with g values similar to the literature values for Li$^+$@$C_{60}^{\bullet-}$ (g = 2.0006)[49] and $C_{20}H_{10}^{\bullet-}$ (g = 2.0027).[50] Thus, the spin state of the CS state can be assigned to be triplet ^{3}($C_{20}H_{10}^{\bullet+}$/Li$^+$@$C_{60}^{\bullet-}$). From the zero-field splitting value (D = 24 G), the distance (r) between two electron spins was estimated to be 11 Å by using eq 7:

$$D = \frac{3g\beta}{2r^3} = \frac{27800}{r^3} \quad (7)$$

where β is the Bohr magneton.[39,42a,51] This r value is close to the end-to-end distance between Li$^+$@C_{60} and $C_{20}H_{10}$ moieties calculated by the DFT optimized structure of $C_{20}H_{10}$/Li$^+$@C_{60} complex (11 Å) and larger than the center-to-center distance (7.4 Å) in Figure 2. Thus, the distance between $C_{20}H_{10}^{\bullet+}$ and Li$^+$@$C_{60}^{\bullet-}$ in the triplet CS state in PhCN might be somewhat longer than the distance in the ground-state CT complex.

Based on the results described above, the energy diagram of photoinduced ET and BET of the $C_{20}H_{10}$/Li$^+$@C_{60} system is shown in Scheme 3. Photoexcitation of the CT complex formed

Scheme 3. Energy Diagram of Photoinduced ET and BET in the $C_{20}H_{10}$/Li$^+$@C_{60} System[a]

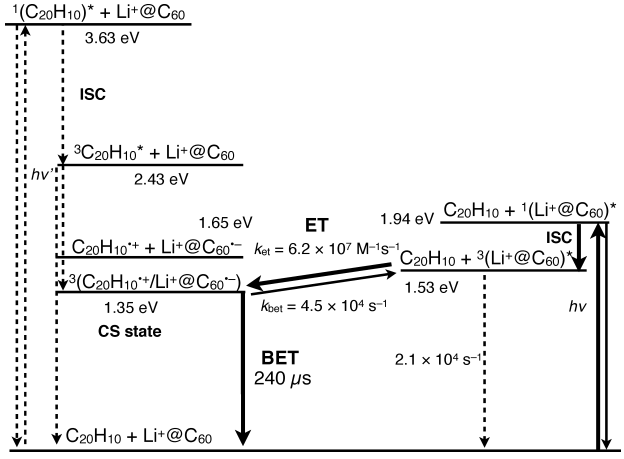

[a]Broken arrow: minor pathway.

between corannulene and Li$^+$@C_{60} resulted in formation of the singlet CS state, ^{1}($C_{20}H_{20}^{\bullet+}$/Li$^+$@$C_{60}^{\bullet-}$), which decayed to the ground state with a decay rate constant of (7.4 ± 0.1) × 10^8 s^{-1}. In contrast, photoinduced intermolecular ET from $C_{20}H_{10}$ to the triplet excited state [^{3}(Li$^+$@C_{60})*] resulted in formation of the triplet CS state, ^{3}($C_{20}H_{10}^{\bullet+}$/Li$^+$@$C_{60}^{\bullet-}$), which is lower in energy than ^{3}(Li$^+$@C_{60})*. The BET from Li$^+$@$C_{60}^{\bullet-}$ to $C_{20}H_{10}^{\bullet+}$ in the triplet CS state to the ground state occurred with a remarkably long lifetime (240 μs) due to the spin-forbidden process and also due to the larger driving force than λ = 1.04 eV ($-\Delta G_{BET}$ = 1.35 eV) which is in the Marcus inverted region.

CONCLUSION

In summary, we have successfully demonstrated that a CT complex was formed between $C_{20}H_{10}$ and Li$^+$@C_{60} in the ground state by the concave−convex π−π CT interaction. Although the singlet CS state produced upon photoexcitation of the CT complex has a short lifetime of 1.4 ns, photoinduced ET from $C_{20}H_{10}$ to ^{3}(Li$^+$@C_{60})* resulted in formation of the triplet CS state, which stayed intact to attain a long lifetime of 240 μs in PhCN. Such a long CS lifetime results from the small electronic coupling term (V = 0.0080 cm^{-1}) and the spin-forbidden BET process. The long-lived charge separation between corannulene and Li$^+$@C_{60} using concave−convex π−π CT interaction between two curved π-surfaces revealed in this study paves a new way for development of efficient CS systems of Li$^+$@C_{60}, which would not be possible by using pristine C_{60}.

EXPERIMENTAL SECTION

Materials. Chemicals were commercially purchased and used without further purification, unless otherwise noted. Lithium ion-encapsulated fullerene hexafluorophosphate (Li$^+$@$C_{60}PF_6^-$: 96%) provided by Idea International Co. Ltd. was commercially obtained from Wako Pure Chemicals, Co. Ltd., Japan and used without further purification. The purity was confirmed by the data including elemental analysis, LDI-TOF-MS, ICP, etc. examined for each lot of the product by the company. Corannulene was synthesized according to the literature.[52] Acetonitrile (MeCN) was purchased from Wako Pure

dx.doi.org/10.1021/ja505391x | J. Am. Chem. Soc. 2014, 136, 13240−13248

Chemical as a spectral grade and used as received. PhCN was purified by distillation over P_2O_5 *in vacuo*.[53]

Absorption Spectral Measurements. Absorption spectra were recorded on a JASCO V-670 and a Hewlett-Packard 8453 diode array spectrophotometers. The titration of $Li^+@C_{60}PF_6^-$ with $C_{20}H_{10}$ was performed as follows. An initial volume of 0.6 mL of a 0.1 mM solution of $Li^+@C_{60}PF_6^-$ in PhCN was placed in a 2 mm cell. A solution of $C_{20}H_{10}$ (200 mM) and $Li^+@C_{60}PF_6^-$ (0.1 mM) in PhCN was subsequently added, and the absorption spectrum was recorded after each addition. $Li^+@C_{60}PF_6^-$ was added into a mother solution of $C_{20}H_{10}$ to avoid dilution effects.

NMR Measurements. ^{7}Li NMR spectra were measured on an AVANCE 600 spectrometers at 298 K. NMR spectra are calibrated with LiCl (D_2O) = 0 ppm as an external standard. ^{7}Li NMR of $Li^+@C_{60}PF_6^-$ without/with $C_{20}H_{10}$ was performed as follows. ^{7}Li NMR of 1.0 mM solution of $Li^+@C_{60}PF_6^-$ in *o*-dichlorobenzene-d_4 (0.6 mL) was measured and then LiCl in D_2O with the same parameters. After addition of 10 equiv of $C_{20}H_{10}$ as a 60 mM *o*-dichlorobenzene-d_4 solution (11.7 mL), ^{7}Li NMR was measured again.

Emission Spectral Measurements. Emission of $C_{20}H_{10}$ was measured on a Horiba FluoroMax-4 spectrofluorophotometer. Phosphorescence of $C_{20}H_{10}$ was measured in a 2-methyltetrahydrofuran glass at 77 K under the deaerated conditions. The sample tube (3 mm diameter) was put in a quartz liquid nitrogen Dewar flask. The excitation wavelength was at 300 nm. Fluorescence was measured in deaerated PhCN of $C_{20}H_{10}$ excited at 300 nm. The solutions were degassed by nitrogen bubbling for 15 min prior to the measurements.

Laser Flash Photolysis Measurements. Femtosecond transient absorption spectroscopy experiments were conducted using an ultrafast source: Integra-C (Quantronix Corp.) and a commercially available optical detection system: Helios provided by Ultrafast Systems LLC. Nanosecond time-resolved transient absorption measurements were carried out using the laser system provided by UNISOKU Co., Ltd. The detailed instrumentations are given in SI.

Electrochemical Measurements. CV and SHACV measurements were performed with an ALS630B electrochemical analyzer. The platinum working electrode (BAS, surface i.d. 1.6 mm) was polished with alumina suspension and rinsed with PhCN before use. The counter electrode was a platinum wire (0.5 mm dia.). The measured potentials were recorded with respect to an $Ag/AgNO_3$ (0.01 M) reference electrode. The values of redox potentials (vs $Ag/AgNO_3$) are converted into those vs SCE by addition of 0.29 V.[54]

EPR Measurements. EPR spectra were taken on a JEOL X-band spectrometer (JES-RE1XE). EPR spectra of the CS state of $C_{20}H_{10}/Li^+@C_{60}$ in PhCN were measured under photoirradiation for a PhCN glass containing $C_{20}H_{10}/Li^+@C_{60}$ (5.0 mM/0.5 mM) at 4 K with a high-pressure mercury lamp (USH-1005D) through a water filter focusing at the sample cell in the EPR cavity. The *g* value was calibrated using an Mn^{2+} marker.

Theoretical Calculations. Density functional theory calculations were performed on a 32CPU workstation (PQS, Quantum Cube QS8−2400C-064). Geometry optimizations were carried out using the B3LYP/6-31G(d) level of theory for $C_{20}H_{10}$, $Li^+@C_{60}$, and $C_{20}H_{10}/Li^+@C_{60}$ complex as implemented in the Gaussian 09 program revision A.02.[36]

■ ASSOCIATED CONTENT

Supporting Information

Spectral data (Figures S1−S11), kinetic parameters (Tables S1−S3), and full author list for refs 33b, 34, and 36a. This material is available free of charge via the Internet at http://pubs.acs.org.

■ AUTHOR INFORMATION

Corresponding Author

fukuzumi@chem.eng.osaka-u.ac.jp

Notes

The authors declare no competing financial interest.

■ ACKNOWLEDGMENTS

This work was supported by JSPS (nos. 12J10461 to M.Y. and 23750014, 26620154, 26288037 to K.O.) and an ALCA project from JST, Japan.

■ REFERENCES

(1) (a) *The Photosynthetic Reaction Center*; Deisenhofer, J., Norris, J. R., Eds.; Academic Press: San Diego, 1993. (b) *Molecular Level Artificial Photosynthetic Materials*; Meyer, G. J., Ed.; John Wiley & Sons: New York, 1997.

(2) (a) Frey, J.; Kodis, G.; Straight, S. D.; Moore, T. A.; Moore, A. L.; Gust, D. *J. Phys. Chem. A* **2013**, *117*, 607−615. (b) Gust, D.; Moore, T. A.; Moore, A. L. In *Electron Transfer in Chemistry*; Balzani, V., Ed.; Wiley-VCH: Weinheim, 2001, Vol. 3, pp 272−336. (c) Gust, D.; Moore, T. A.; Moore, A. L. *Acc. Chem. Res.* **1993**, *26*, 198−205. (d) Gust, D.; Moore, T. A.; Moore, A. L. *Acc. Chem. Res.* **2009**, *42*, 1890−1898.

(3) (a) Ricks, A. B.; Brown, K. E.; Wenninger, M.; Karlen, S. D.; Berlin, Y. A.; Co, D. T.; Wasielewski, M. R. *J. Am. Chem. Soc.* **2012**, *134*, 4581−4588. (b) Lewis, F. D.; Letsinger, R. L.; Wasielewski, M. R. *Acc. Chem. Res.* **2001**, *34*, 159−170. (c) Wasielewski, M. R. *Acc. Chem. Res.* **2009**, *42*, 1910−1921.

(4) (a) Faiz, J. A.; Heitz, V.; Sauvage, J.-P. *Chem. Soc. Rev.* **2009**, *38*, 422−442. (b) Diederich, F.; Gómez-López, M. *Chem. Soc. Rev.* **1999**, *28*, 263−277. (c) Chambron, J.-C.; Collin, J.-P.; Dalbavie, J.-O.; Dietrich-Buchecker, C. O.; Heitz, V.; Odobel, F.; Solladié, N.; Sauvage, J.-P. *Coord. Chem. Rev.* **1998**, *178*−*180*, 1299−1312.

(5) (a) Bottari, G.; De la Torre, G.; Guldi, D. M.; Torres, T. *Chem. Rev.* **2010**, *110*, 6768−6816. (b) D'Souza, F.; Ito, O. *Chem. Soc. Rev.* **2012**, *41*, 86−96. (c) Balzani, V. *Coord. Chem. Rev.* **2001**, *219*−*221*, 545−572.

(6) (a) Fukuzumi, S. *Org. Biomol. Chem.* **2003**, *1*, 609−620. (b) Fukuzumi, S. *Phys. Chem. Chem. Phys.* **2008**, *10*, 2283−2297. (c) Fukuzumi, S.; Ohkubo, K. *J. Mater. Chem.* **2012**, *22*, 4575−4587. (d) Fukuzumi, S.; Ohkubo, K.; Suenobu, T. *Acc. Chem. Res.* **2014**, *47*, 1455−1464.

(7) (a) Kirner, S.; Sekita, M.; Guldi, D. M. *Adv. Mater.* **2014**, *26*, 1482−1493. (b) Fukuzumi, S.; Guldi, D. M. In *Electron Transfer in Chemistry*; Balzani, V., Ed.; Wiley-VCH: Weinheim, 2001, Vol. 2, pp 270−337.

(8) (a) Kawashima, Y.; Ohkubo, K.; Fukuzumi, S. *J. Phys. Chem. A* **2013**, *117*, 6737−6743. (b) Wrobel, D.; Graja, A. *Coord. Chem. Rev.* **2011**, *255*, 2555−2577.

(9) (a) D'Souza, F.; Ito, O. *Chem. Soc. Rev.* **2012**, *41*, 86−96. (b) Fukuzumi, S.; Ohkubo, K.; D'Souza, F.; Sessler, J. L. *Chem. Commun.* **2012**, *48*, 9801−9815. (b) D'Souza, F.; Ito, O. *Chem. Commun.* **2009**, 4913−4928. (c) Chitta, R.; D'Souza, F. *J. Mater. Chem.* **2008**, *18*, 1440−1471.

(10) (a) Guldi, D. M.; Costa, R. D. *J. Phys. Chem. Lett.* **2013**, *4*, 1489−1501. (b) Bottari, G.; Trukhina, O.; Ince, M.; Torres, T. *Coord. Chem. Rev.* **2012**, *256*, 2453−2477.

(11) (a) Costa, R. D.; Lodermeyer, F.; Casillas, R.; Guldi, D. M. *Energy Environ. Sci.* **2014**, *7*, 1281−1296. (b) Guldi, D. M.; Sgobba, V. *Chem. Commun.* **2011**, *47*, 606−610.

(12) (a) Shen, Y.; Nakanishi, T. *Phys. Chem. Chem. Phys.* **2014**, *16*, 7199−7204. (b) Fukuzumi, S.; Ohkubo, K. *Dalton Trans.* **2013**, *42*, 15846−15858. (c) Babu, S. S.; Moehwald, H.; Nakanishi, T. *Chem. Soc. Rev.* **2010**, *39*, 4021−4035. (d) Guldi, D. M.; Illescas, B. M.; Atienza, C. M.; Wielopolski, M.; Martin, N. *Chem. Soc. Rev.* **2009**, *38*, 1587−1597.

(13) (a) Wang, T.; Pearson, A. J.; Lidzey, D. G. *J. Mater. Chem. C* **2013**, *1*, 7266−7293. (b) Jariwala, D.; Sangwan, V. K.; Lauhon, L. J.; Marks, T. J.; Hersam, M. C. *Chem. Soc. Rev.* **2013**, *42*, 2824−2860. (c) Dubacheva, G. V.; Liang, C.-K.; Bassani, D. M. *Coord. Chem. Rev.* **2012**, *256*, 2628−2639.

(14) (a) Mulliken, R. S.; Person, W. B. *Molecular Complexes, a Lecture and Reprint Vol.*; Wiley-Interscience: New York, 1969. (b) Foster, R. *Organic Charge Transfer Complexes*; Academic Press: New York, 1969.

(c) Fukuzumi, S.; Wong, C. L.; Kochi, J. K. *J. Am. Chem. Soc.* **1980**, *102*, 2928−2939.
(15) (a) Canevet, D.; Gallego, M.; Isla, H.; de Juan, A.; Pérez, E. M.; Martín, N. *J. Am. Chem. Soc.* **2011**, *133*, 3184−3190. (b) Canevet, D.; Peréz, E. M.; Martín, N. *Angew. Chem., Int. Ed.* **2011**, *50*, 9248−9259. (b) Huerta, E.; Isla, H.; Pérez, E. M.; Bo, C.; Martín, N.; de Mendoza, J. *J. Am. Chem. Soc.* **2010**, *132*, 5351−5353.
(16) Zhou, Z.; Qin, Y.; Xu, W.; Zhu, D. *Chem. Commun.* **2014**, *50*, 4082−4084.
(17) (a) Isla, H.; Grimm, B.; Pérez, E. M.; Torres, M. R.; Herranz, M. A.; Viruela, R.; Juan Aragó, J.; Ortí, E.; Guldi, D. M.; Martín, N. *Chem. Sci.* **2012**, *3*, 498−508. (b) Pérez, E. M.; Capodilupo, A. L.; Fernández, G.; Sánchez, L.; Viruela, P. M.; Viruela, R.; Ortí, E.; Bietti, M.; Martín, N. *Chem. Commun.* **2008**, 4567−4569.
(18) (a) Kawase, T.; Tanaka, K.; Fujiwara, N.; Darabi, H. R.; Oda, M. *Angew. Chem., Int. Ed.* **2003**, *42*, 1624−1628. (b) Kawase, T.; Seirai, Y.; Darabi, H. R.; Oda, M.; Sarakai, Y.; Tashiro, K. *Angew. Chem., Int. Ed.* **2003**, *42*, 1621−1624.
(19) Iwamoto, T.; Watanabe, Y.; Takaya, H.; Haino, T.; Yasuda, N.; Yamago, S. *Chem.−Eur. J.* **2013**, *19*, 1406−14068.
(20) Nakanishi, Y.; Omachi, H.; Matsuura, S.; Miyata, Y.; Ryo Kitaura, R.; Segawa, Y.; Itami, K.; Shinohara, H. *Angew. Chem., Int. Ed.* **2014**, *53*, 3102−3106.
(21) Isobe, H.; Hitosugi, S.; Yamasaki, T.; Iizuka, R. *Chem. Sci.* **2013**, *4*, 1293−1297.
(22) (a) Kishi, N.; Akita, M.; Yoshizawa, M. *Angew. Chem., Int. Ed.* **2014**, *53*, 3604−3607. (b) Kishi, N.; Akita, M.; Kamiya, M.; Hayashi, S.; Hsu, H.-F.; Yoshizawa, M. *J. Am. Chem. Soc.* **2013**, *135*, 12976−12979.
(23) Filatov, A. S.; Ferguson, M. V.; Spisak, S. N.; Li, B.; Campana, C. F.; Petrukhina, M. A. *Cryst. Growth Design* **2014**, *14*, 756−762.
(24) Grimm, B.; Santos, J.; Illescas, B. M.; Munoz, A.; Guldi, D. M.; Martín, N. *J. Am. Chem. Soc.* **2010**, *132*, 17387−17389.
(25) (a) Barth, W. E.; Lawton, R. G. *J. Am. Chem. Soc.* **1966**, *88*, 380−381. (b) Barth, W. E.; Lawton, R. G. *J. Am. Chem. Soc.* **1971**, *93*, 1730−1745.
(26) (a) Wu, Y.-T.; Siegel, J. S. *Chem. Rev.* **2006**, *106*, 4843−4867. (b) *Fragments of Fullerenes and Carbon Nanotubes: Designed Synthesis, Usual Reactions, and Coordination Chemistry*; Petrukhina, M. A., Scott, L. T., Eds.; John Wiley & Sons: Hoboken, NJ, 2012. (c) Scott, L. T.; Cheng, P.-C.; Hashemi, M. M.; Bratcher, M. S.; Meyer, D. T.; Warren, H. B. *J. Am. Chem. Soc.* **1997**, *119*, 10963−10968. (d) Tsefrikas, V. M.; Scott, L. T. *Chem. Rev.* **2006**, *106*, 4868−4884.
(27) (a) Sygula, A. *Eur. J. Org. Chem.* **2011**, *9*, 1611−1625. (b) Allemann, O.; Duttwyler, S.; Romanato, P.; Baldridge, K. K.; Siegel, J. S. *Science* **2011**, *332*, 574−577. (c) Schmidt, B. M.; Seki, S.; Topolinski, B.; Ohkubo, K.; Fukuzumi, S.; Sakurai, H.; Lentz, D. *Angew. Chem., Int. Ed.* **2012**, *51*, 11385−11388. (d) Schmidt, B. M.; Topolinski, B.; Yamada, M.; Higashibayashi, S.; Shionoya, M.; Sakurai, H.; Lentz, D. *Chem.−Eur. J.* **2013**, *19*, 13872−13880. (e) Pedersen, S. U.; Christensen, T. B.; Thomasen, T.; Daasbjerg, K. *J. Electroanal. Chem.* **1998**, *454*, 123−143.
(28) (a) Scott, L. T.; Hashemi, M. M.; Bratcher, M. S. *J. Am. Chem. Soc.* **1992**, *114*, 1920−1921. (b) Seiders, T. J.; Baldridge, K. K.; Grube, G. H.; Siegel, J. S. *J. Am. Chem. Soc.* **2001**, *123*, 517−525. (c) Eisenberg, D.; Quimby, J. M.; Scott, L. T.; Schenhar, R. *J. Phys. Org. Chem.* **2013**, *26*, 124−130.
(29) (a) Lovas, F. J.; McMahon, R. J.; Grabow, J.-U.; Schnell, M.; Mack, J.; Scott, L. T.; Kuczkowski, R. L. *J. Am. Chem. Soc.* **2005**, *127*, 4345−4349. (b) Li, J.; Liu, Y.; Qian, Y.; Li, L.; Xie, L.; Shang, J.; Yu, T.; Yi, M.; Huang, W. *Phys. Chem. Chem. Phys.* **2013**, *15*, 12694−12701.
(30) (a) Filatov, A. S.; Petrukhina, M. A. *Coord. Chem. Rev.* **2010**, *254*, 2234−2246. (b) Petrukhina, M. A.; Scott, L. T. *Dalton Trans.* **2005**, 2964−2075. (c) Zabula, A. V.; Filatov, A. S.; Spisak, S. N.; Rogachev, A. Yu.; Petrukhina, M. A. *Science* **2011**, *333*, 1008−1011. (d) Topolinski, B.; Schmidt, B. M.; Kathan, M.; Troyanov, S. I.; Lentz, D. *Chem. Commun.* **2012**, *48*, 6298−6300. (e) Lee, H. B.; Sharp, P. R. *Organometallics* **2005**, *24*, 4875−4877. (f) Yamada, M.; Tashiro, S.; Miyake, R.; Shionoya, M. *Dalton Trans.* **2013**, *42*, 3300−3303. (g) Spisak, S. N.; Zabula, A. V.; Ferguson, M. V.; Filatov, A. S.; Petrukhina, M. A. *Organometallics* **2013**, *32*, 538−543.
(31) (a) Becker, H.; Javahery, G.; Petrie, S.; Cheng, P.-C.; Schwarz, H.; Scott, L. T.; Bohme, D. K. *J. Am. Chem. Soc.* **1993**, *115*, 11636−11637. (b) Dawe, L. N.; Alhujran, T. A.; Tran, H.-A.; Mercer, J. I.; Jackson, E. A.; Scott, L. T.; Georghiou, P. E. *Chem. Commun.* **2012**, *48*, 5563−5565. (c) Xiao, W.; Passerone, D.; Ruffieux, P.; Aït-Mansour, K.; Gröning, O.; Tosatti, E.; Siegel, J. S.; Fasel, R. *J. Am. Chem. Soc.* **2008**, *130*, 4767−4771. (d) Sygula, A.; Fronczek, F. R.; Sygula, R.; Rabideau, P. W.; Olmstead, M. M. *J. Am. Chem. Soc.* **2007**, *129*, 3842−3843. (e) Heorghiou, P. E.; Tran, A. H.; Mizyed, S.; Bancu, M.; Scott, L. T. *J. Org. Chem.* **2005**, *70*, 6158−6163. (f) Yanney, M.; Sygula, A. *Tetrahedron Lett.* **2013**, *54*, 2604−2607. (g) Stuparu, M. C. *Angew. Chem., Int. Ed.* **2013**, *52*, 7786−7790.
(32) Kawase, T.; Kurata, H. *Chem. Rev.* **2006**, *106*, 5250−5273.
(33) For ET reactions of coronenes, see: (a) Whalley, A. C.; Plunkett, K. N.; Gorodetsky, A. A.; Schenck, C. L.; Chiu, C.-Y.; Steigerwald, M. L.; Nuckolls, C. *Chem. Sci.* **2011**, *2*, 132−135. (b) Tremblay, N. J.; et al. *ChemPhysChem* **2010**, *11*, 799−803 (full author list is given in SI).
(34) Aoyagi, S.; et al. *Nat. Chem.* **2010**, *2*, 678−683 (full author list is given in SI).
(35) Benesi, H. A.; Hildebrand, J. H. *J. Am. Chem. Soc.* **1949**, *71*, 2703−2707.
(36) (a) Frisch, M. J. et al. *Gaussian 09*, revision A.02, Gaussian, Inc.: Wallingford CT, 2009 (full author list is given in SI). (b) Becke, A. D. *J. Chem. Phys.* **1993**, *98*, 5648−5652. (c) Lee, C.; Yang, W.; Parr, R. G. *Phys. Rev. B* **1988**, *37*, 785−789.
(37) (a) McCord, T. G.; Smith, D. E. *Anal. Chem.* **1969**, *41*, 1423−1441. (b) Bond, A. M.; Smith, D. E. *Anal. Chem.* **1974**, *46*, 1946−1951. (c) Wasielewski, M. R.; Bleslow, R. *J. Am. Chem. Soc.* **1976**, *98*, 4222−4229. (d) Arnett, E. M.; Amarnath, K.; Harvey, N. G.; Cheng, J.-P. *J. Am. Chem. Soc.* **1992**, *112*, 344−355. (e) Fukuzumi, S.; Ohkubo, K.; Imahori, H.; Guldi, D. M. *Chem.−Eur. J.* **2003**, *9*, 1585−1593.
(38) Kawashima, Y.; Ohkubo, K.; Fukuzumi, S. *J. Phys. Chem. A* **2012**, *116*, 8942−8928.
(39) Kawashima, Y.; Ohkubo, K.; Mase, K.; Fukuzumi, S. *J. Phys. Chem. C* **2013**, *117*, 21166−21177.
(40) (a) Mulliken, R. S. *J. Am. Chem. Soc.* **1950**, *72*, 600−608. (b) Mulliken, R. S. *J. Am. Chem. Soc.* **1952**, *74*, 811−824.
(41) (a) Catalán, J.; Elguero, J. *J. Am. Chem. Soc.* **1993**, *115*, 9249−9252. (b) Fujitsuka, M.; Yahata, Y.; Watanabe, A.; Ito, O. *Polymer* **2000**, *41*, 2807−2812. (c) Guldi, D. M.; Hungerbühler, H.; Charmichael, I. *J. Phys. Chem. A* **2000**, *104*, 8601−8608.
(42) (a) Fukuzumi, S.; Ohkubo, K.; Kawashima, Y.; Kim, D. S.; Park, J. S.; Jama, A.; Lynch, V. M.; Kim, D.; Sessler, J. L. *J. Am. Chem. Soc.* **2011**, *133*, 15938−15941. (b) Yamaji, M.; Takehira, K.; Mikoshiba, T.; Tojo, S.; Okada, Y.; Fujitsuka, M.; Majima, T.; Tobita, S.; Nishimura, J. *Chem. Phys. Lett.* **2006**, *425*, 53−57.
(43) Arbogast, J. W.; Foote, C. S.; Kao, M. *J. Am. Chem. Soc.* **1992**, *114*, 2277−2279.
(44) (a) Marcus, R. A. *J. Phys. Chem.* **1956**, *24*, 966−978. (b) Marcus, R. A. *Annu. Rev. Phys. Chem.* **1964**, *15*, 155−196. (c) Marcus, R. A. *Angew. Chem., Int. Ed.* **1993**, *32*, 1111−1121.
(45) For small temperature dependence of the ET rate constant, see: (a) Liang, N.; Miller, J. R.; Closs, G. L. *J. Am. Chem. Soc.* **1990**, *112*, 5353−5354. (b) Chen, P.; Mecklenburg, S. L.; Meyer, T. J. *J. Phys. Chem.* **1993**, *97*, 13126−13131. (c) Smitha, M. A.; Gopidas, K. R. *Chem. Phys. Lett.* **2001**, *350*, 86−92. (d) Scott, A. M.; Wasielewski, M. R. *J. Am. Chem. Soc.* **2011**, *133*, 3005−3013.
(46) (a) Kamimura, T.; Ohkubo, K.; Kawashima, Y.; Nobukuni, H.; Naruta, Y.; Tani, F.; Fukuzumi, S. *Chem. Sci.* **2013**, *4*, 1451−1461. (b) Ohkubo, K.; Kawashima, Y.; Fukuzumi, S. *Chem. Commun.* **2012**, *48*, 4314−4316.
(47) (a) Bill, N. L.; Ishida, M.; Kawashima, Y.; Ohkubo, K.; Sung, Y. M.; Lynch, V. M.; Lim, J. M.; Kim, D.; Sessler, J. L.; Fukuzumi, S. *Chem. Sci.* **2014**, *5*, 3888−3896. (b) Davis, C. M.; Kawashima, Y.; Ohkubo, K.; Lim, J. M.; Kim, D.; Fukuzumi, S.; Sessler, J. L. *J. Phys.*

Chem. C **2014**, *118*, 13503−13513. (c) Sessler, J. L.; Karnas, E.; Kim, S. K.; Ou, Z.; Zhang, M.; Kadish, K. M.; Ohkubo, K.; Fukuzumi, S. *J. Am. Chem. Soc.* **2008**, *130*, 15256−15257. (d) Tanaka, M.; Ohkubo, K.; Gros, C. P.; Guilard, R.; Fukuzumi, S. *J. Am. Chem. Soc.* **2006**, *128*, 14625−14633. (e) Honda, T.; Nakanishi, T.; Ohkubo, K.; Kojima, T.; Fukuzumi, S. *J. Am. Chem. Soc.* **2010**, *132*, 10155−10163. (f) Ohkubo, K.; Mase, K.; Karnas, E.; Sessler, J. L.; Fukuzumi, S. *J. Phys. Chem. C* **2014**, *118*, 18436−18444.

(48) Suzuki, S.; Sugimura, R.; Kozaki, M.; Keyaki, K.; Nozaki, K.; Ikeda, N.; Akiyama, K.; Okada, K. *J. Am. Chem. Soc.* **2009**, *131*, 10374−10375.

(49) Ueno, H.; Kokubo, K.; Nakamura, Y.; Ohkubo, K.; Ikuma, N.; Moriyama, H.; Fukuzumi, S.; Oshima, T. *Chem. Commun.* **2013**, *49*, 7376−7378.

(50) Janata, J.; Gendell, J.; Ling, C.-Y.; Barth, W. E.; Backes, L.; Mark, H. B.; Lawton, R. G. *J. Am. Chem. Soc.* **1967**, *89*, 3056−3058.

(51) Park, J. S.; Karnas, E.; Ohkubo, K.; Chen, P.; Kadish, K. M.; Fukuzumi, S.; Bielawski, C. W.; Hudnall, T. W.; Lynch, V. M.; Sessler, J. L. *Science* **2010**, *329*, 1324−1327.

(52) (a) Butterfield, A. M.; Gilomen, B.; Siegel, J. S. *Org. Process Rev. Dev.* **2012**, *16*, 664−676. (b) Borchardt, A.; Fuchicello, A.; Kilway, K. V.; Baldrige, K. K.; Siegel, J. S. *J. Am. Chem. Soc.* **1992**, *114*, 1921−1923. (c) Christoffers, J.; Mann, A. *Eur. J. Org. Chem.* **1999**, 2511−2514. (d) Walinska-Mocydlarz, J.; Canonne, P.; Leitch, L. C. *Synthesis* **1974**, 566−568. (e) Jones, C. S.; Elliot, E.; Siegel, J. S. *Synlett* **2004**, 187−191. (f) Guillermet, O.; Niemi, E.; Nagarajan, S.; Bouju, X.; Martrou, D.; Gourdon, A.; Gauthier, S. *Angew. Chem., Int. Ed.* **2009**, *48*, 1970−1973. (g) Seiders, T. J.; Elliott, E. L.; Grube, G. H.; Siegel, J. S. *J. Am. Chem. Soc.* **1999**, *121*, 7804−7813. (h) Sygula, A.; Rabideau, P. W. *J. Am. Chem. Soc.* **2000**, *122*, 6323−6324.

(53) Armarego, W. L. F.; Chai, C. L. L. In *Purification of Laboratory Chemicals*, 6th ed.; Pergamon Press: Oxford, 2009.

(54) Mann, C. K.; Barnes, K. K. In *Electrochemical Reactions in Non-aqueous Systems*; Mercel Dekker: New York, 1970.